Visnyk NTUU KPI Seriia – Radiotekhnika Radioaparatobuduvannia, 2026, Iss. 103, pp. 85–93

UDC 621.384.3

Model of Infrared Radiation Polarization of a Drone

Kolobrodov V. G.

National Technical University of Ukraine "Ihor Sikorsky Kyiv Polytechnic Institute", Kyiv, Ukraine

E-mail: *thermo@ukr.net*

A physico-mathematical model of infrared (IR) radiation polarization from a drone, which can be used in the creation of polarimetric thermal imagers (PTI) for detection and recognition of surveillance objects, is developed. *Analysis of Research.* Thermal imaging systems are widely used, primarily in military applications, such as in the thermal cameras of drones. The principle of operation of classical thermal imagers is based on converting the brightness of IR radiation from the observed object and background from the plane of objects into an appropriate distribution of background-target scene (BTS) brightness on a display screen within the visible spectrum. If the contrast is low or absent, it becomes impossible to detect such an object. Current models do not simultaneously account for the drone's emission and reflected radiation, leading to errors in the detection range estimation. The use of polarization properties of radiation allows solving this problem. Therefore, developing and researching a model of IR radiation polarization from the drone is a very important task for creating promising PTI for drone detection. *Unresolved parts of the overall problem* include the lack of a model that considers both emission and reflected polarization simultaneously. *The purpose of the article* is to develop a physico-mathematical model of IR radiation polarization from a drone, which can be used in the creation of PTI systems designed for drone detection and recognition. *Research material presentation* — the drone is modeled as a flat plate characterized by an reflection coefficient and a complex refractive index, which allowed the development of methods for calculating parameters of elliptically polarized radiation. *Analysis of the developed methods* indicates that for modeling the polarization state of the observed object's radiation, it is appropriate to select the image intensity, degree of polarization, and polarization angle, all determined by the Stokes parameters. *Comparison of obtained results* with those from other researchers involves scientifically substantiating that the polarization of IR radiation from objects and backgrounds, due to their own and reflected radiation, has an opposite character, which significantly worsens the overall degree of polarization. *Conclusions from this research.* The obtained results are relevant for developing a test object model, necessary for designing PTI systems. Future prospects include conducting experimental measurements of IR radiation polarization from real drones and atmospheric conditions, which will help refine the test object parameters.

Keywords: thermal imager; polarization; degree of polarization; emission thermal radiation; reflected thermal radiation

DOI: 10.64915/RADAP.2026.103.85-93

1 Introduction

Thermal imaging monitoring systems (TIMS) are widely used, primarily in military applications, for example, as thermal imaging cameras on drones, as well as in various fields of science and technology [1–3].

The principle of operation of classical thermal imagers is based on the conversion of the brightness (intensity) of the radiation of the object under observation and the background from the plane of objects into an adequate distribution of the brightness of the background-target situation (BTS) image on the display screen. The limiting characteristics of such thermal imagers are determined by the radiation contrast of the BTS. In recent years, developers have been actively trying to use the polarization properties of the radiation components of the BTS to significantly improve these characteristics. As a rule, the radiation from a drone is partially polarized, while that from the background (atmosphere) is natural [4–6]. Thus, under certain conditions, polarimetric images allow the signal from the target to be increased and the signal from background interference to be reduced.

The main characteristics of polarized radiation are intensity, degree of polarization, azimuth, and ellipticity of polarization [6–8]. These characteristics are determined by the physical processes of radiation from the surface of drones due to their own radiation and reflection of external radiation, as well as their own radiation and scattering of the atmosphere. Polarimetric thermal imagers (PTI) are used to measure these characteristics in the infrared (IR) region of the

spectrum. To create a PTI, it is necessary to know the physical and mathematical model of polarized radiation of the BTS. There is practically no information about such models in scientific and technical literature. Therefore, the development and research of a model of infrared radiation polarization of a drone is a very important task for the creation of promising PTI for drone detection.

Problem statement

The purpose of this article is to develop and research a physical and mathematical model of polarized infrared radiation from a drone, which can be used in the creation of polarimetric thermal imagers designed to detect and recognize drones.

2 Main characteristics of polarized radiation

There are two main theories underlying radiation polarization: Fresnel's theory and Kirchhoff's law, which are determined solely by the refractive indices of the media. In physical optics, depending on the orientation of the electric field intensity vector $\vec{E}$, the types of polarization are considered: natural, linear, partially polarized, elliptical, and circular (Fig. 1) [7,8]:

- *Natural polarization* occurs when the vector $\vec{E}$ has an equally probable orientation in a plane perpendicular to the direction of propagation of the beam.
- *Linear or plane-polarized light*, when the vector $\vec{E}$ oscillates in one plane. The plane passing through the vectors $\vec{E}$ and $\vec{v}$ is named the plane of polarization, where $\vec{v}$ is the vector velocity of radiation propagation, which coincides with the direction of the beam.
- *Partially polarized light* is when the vector $\vec{E}$ has a predominant (more probable) direction of orientation in space.
- *Elliptically polarized light* is when the vector $\vec{E}$ propagates in space along a helical trajectory with variable amplitude, the projection of which onto a plane perpendicular to the direction of the beam describes an ellipse.
- *Circularly polarized light* (polarized in a circle) is a special case of elliptically polarized light, where the ellipse becomes a circle.

To research partially polarized radiation, Stokes proposed converting it into elliptically polarized radiation, describing it using Stokes vector parameters, which allow calculating the parameters of different types of polarization [6–10].

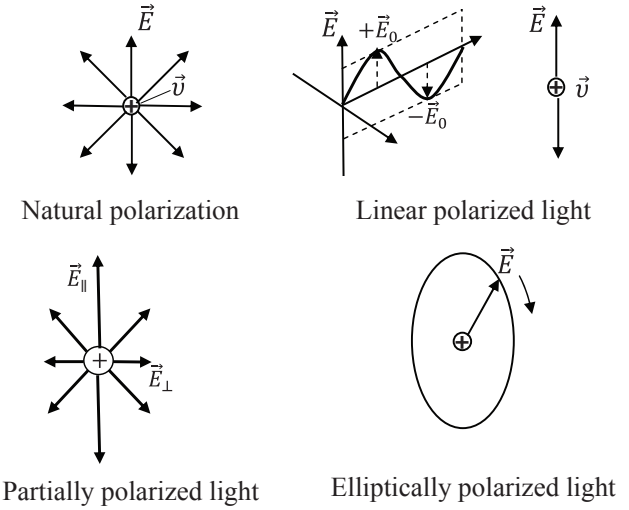

Fig. 1. Main types of light polarization: natural, linear, partially polarized, and elliptical

Figure 2 shows an optical system for obtaining elliptically polarized light. Consider the interaction of two coherent waves that are linearly polarized in mutually perpendicular planes and propagate in the same direction. Natural light normally falls on a polarizer, which forms a linearly polarized wave $\vec{E}_{lp}$ at the output that passes through a phase plate. The plate has an optical axis that is parallel to its surface.

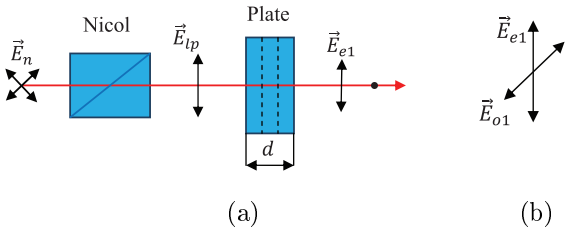

Fig. 2. Diagram for obtaining elliptically polarized light (a) and its vector model (b)

As a result of double refraction in the plate, ordinary and extraordinary rays are formed, which propagate in the same direction and have a phase difference at the plate exit

$$\Delta\varphi = k \cdot \Delta d = \frac{2\pi}{\lambda}(n_o - n_e)d, \qquad (1)$$

where d is the plate thickness; $n_o - n_e$ is the difference in refractive indices of the ordinary and extraordinary rays.

Determine the amplitudes of the ordinary E_{o1} and extraordinary E_{e1} rays at the exit from the plate, if the plane of polarization of the ray E_{lp} falling on the plate forms an angle with the optical axis of the crystal. From Fig. 3, we have

$$E_{o1} = E_{lp}\sin\alpha; \quad E_{e1} = E_{lp}\cos\alpha. \qquad (2)$$

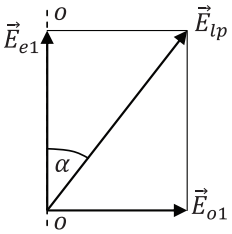

Fig. 3. Vector model of obtaining elliptically polarized light

The amplitudes of ordinary and extraordinary rays vary in time according to the law

$$E_e = E_{e1}\cos\omega t; \quad E_o = E_{o1}\cos(\omega t - \Delta\varphi). \qquad (3)$$

Represent the system of equations (3) in the form of a single equation that does not depend on time t.

$$\frac{E_e}{E_{e1}} = \cos\omega t \ ;$$

$$\frac{E_o}{E_{o1}} = \cos(\omega t - \Delta\varphi) = \cos\omega t\cos\Delta\varphi + \sin\omega t\sin\Delta\varphi =$$

$$= \frac{E_e}{E_{e1}}\cos\Delta\varphi + \sqrt{1-\left(\frac{E_e}{E_{e1}}\right)^2}\sin\Delta\varphi.$$

$$\frac{E_o}{E_{o1}} - \frac{E_e}{E_{e1}}\cos\Delta\varphi = \sqrt{1-\left(\frac{E_e}{E_{e1}}\right)^2}\sin\Delta\varphi,$$

or

$$\left(\frac{E_o}{E_{o1}}\right)^2 - 2\frac{E_o}{E_{o1}}\frac{E_e}{E_{e1}}\cos\Delta\varphi + \left(\frac{E_e}{E_{e1}}\right)^2 = \sin^2\Delta\varphi. \quad (4)$$

Substitute the variables in equation (4): $E_o = x$, $E_{o1} = a$, $E_e = y$, $E_{e1} = b$. Then equation (4):

$$\frac{x^2}{a^2} + \frac{y^2}{b^2} - 2\frac{x}{a}\frac{y}{b}\cos\Delta\varphi = \sin^2\Delta\varphi \ . \quad (4')$$

Equation (4′) represents the equation of an ellipse that is oriented relative to the optical axis oo of the phase plate (Fig. 4). Therefore, the resulting field amplitude at the plate output will form elliptically polarized light. The semi-axes of the ellipse a and b, as well as its orientation, depend on the angle α and the phase difference $\Delta\varphi$ (1).

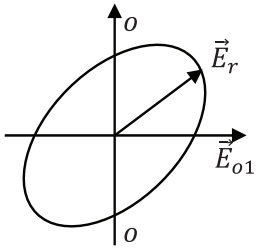

Fig. 4. Vector model of elliptically polarized light

Consider equation (4) for the case when the phase difference $\Delta\varphi$ between the ordinary E_o and extraordinary rays E_e is equal to $\pi/2$. Determine the thickness of the plate that provides this case. From formula (1):

$$\Delta\varphi = \frac{2\pi}{\lambda}(n_o - n_e)d = \frac{\pi}{2}; \Rightarrow d = \frac{\lambda}{4(n_o - n_e)}. \qquad (5)$$

In this case, the difference in path length between the ordinary and extraordinary rays is equal to

$$\Delta d = (n_o - n_e)d = \frac{1}{4}\lambda. \qquad (6)$$

Therefore, a plate made of a single-axis crystal that satisfies condition (5) is called *a plate with a thickness* of $\lambda/4$, or *a quarter-wave plate*.

For such a plate, equations (4) and (4′) (Fig. 4)

$$\frac{E_o^2}{E_{o1}^2} + \frac{E_e^2}{E_{e1}^2} = 1; \qquad \frac{x^2}{a^2} + \frac{y^2}{b^2} = 1. \qquad (7)$$

Expressions (7) represent the equation of an ellipse with semi-axes

$$a = E_{o1} = E_{lp}\sin\alpha; \qquad b = E_{e1} = E_{lp}\cos\alpha. \qquad (8)$$

If α=45°, then $a = b = R$, and equations (7) are transformed into the equation of a circle

$$E_o^2 + E_e^2 = E_{o1}^2; \qquad x^2 + y^2 = R^2. \qquad (9)$$

Therefore, this type of polarization is called *circular* or *circularly polarized*.

To obtain circularly polarized light, it is necessary for linearly polarized light to pass through a quarter-wave plate and α=45°. Due to the principle of reciprocity in optics, circularly polarized light becomes linearly polarized when passing through a quarter-wave plate.

The polarization state of radiation is characterized by intensity I_0, degree of polarization P, ellipticity χ, and polarization angle θ (Fig. 5). The orientation of the ellipse is determined by the polarization angle θ, and the shape of the ellipse is determined by the angle of ellipticity χ. Depending on these angles, elliptically polarized light is converted into linearly polarized light, as well as circularly polarized light with the resulting vector $\vec{E}_r = \vec{E}_o + \vec{E}_e = \vec{x} + \vec{y}$ rotating to the right or left.

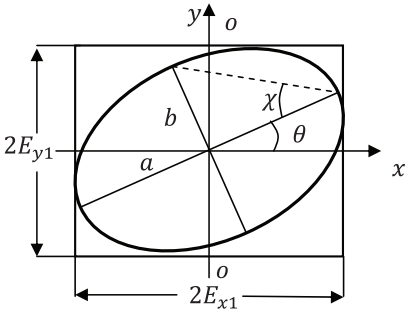

Fig. 5. Radiation parameters for elliptical polarization

The polarization angle θ is the angle between the major axis of the ellipse and the horizontal axis x, which is determined by the components of the electric field of light [7, 8, 10]:

$$tg2\theta = \frac{2E_{0x}E_{0y}\cos\Delta\varphi}{E_{0x}^2 + E_{0y}^2}, \quad \text{where} \quad 0 < \theta < \pi. \qquad (10)$$

The angle of ellipticity χ is given by the ratio of the lengths of the minor and major axes of the ellipse:

$$tg\chi = \frac{\pm b}{a}, \quad \text{where} \quad -\pi/2 < \chi < \pi/2. \qquad (11)$$

The angle of ellipticity χ is also determined by the components of the electric field of radiation:

$$\sin 2\chi = \frac{2E_{0x}E_{0y}\cos\Delta\varphi}{E_{0x}^2 + E_{0y}^2}, \quad \text{where} \quad 0 < \theta < \pi. \qquad (12)$$

3 Polarization of thermal radiation

Researches of the laws of thermal radiation from heated objects show that metal surfaces have a higher degree of radiation polarization compared to dielectric and transparent surfaces. The highest degree of polarization is observed in the radiation of polished surfaces when viewed at a large angle relative to the normal to the surface. This is explained by the laws of radiation refraction at the metal-air interface (Fig. 6).

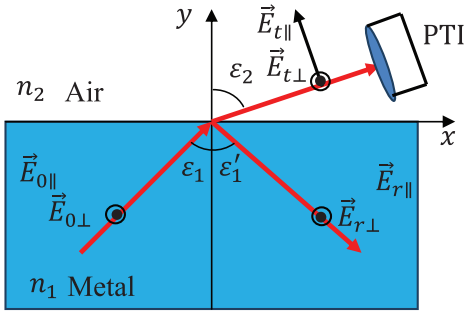

Fig. 6. Radiation and reflection of light falling at an oblique angle ε_1 from metal to the metal-air boundary

According to Kirchhoff's law, the spectral radiation coefficient $\varepsilon(\lambda)$ of the surface of an object under observation, which is in a state of thermal equilibrium, is equal to the absorption coefficient $\alpha(\lambda)$ and is related to the reflection coefficient $R(\lambda)$ by the following ratio [3, 11, 12]:

$$\varepsilon(\lambda) = \alpha(\lambda) = 1 - R(\lambda). \qquad (13)$$

The amplitude of thermal radiation E_t at the metal-air interface is partially polarized, in which the parallel component $E_{t\parallel}$ is smaller than the perpendicular component $E_{t\perp}$ (Fig. 6). The viewing (observation) axis of the PTI is located in the observation plane xy.

Using Kirchhoff's law (13) and Fresnel's formulas for partial energy reflection coefficients $R_\parallel$ and $R_\perp$ [10, 11], we obtain formulas for calculating parallel and perpendicular components (partial) of radiation coefficients [10, 11, 14]:

$$\varepsilon_\parallel = \left|\frac{E_{t\parallel}}{E_{i\parallel}}\right|^2 = \frac{4n_1\cos\varepsilon_2}{(n_1^2+\kappa_1^2)\cos^2\varepsilon_2 + 2n_1\cos\varepsilon_2 + 1}; \qquad (14)$$

$$\varepsilon_\perp = \left|\frac{E_{t\perp}}{E_{i\perp}}\right|^2 = \frac{4n_1\cos\varepsilon_2}{\cos^2\varepsilon_2 + 2n_1\cos\varepsilon_2 + n_1^2 + \kappa_1^2}, \qquad (15)$$

where $n_c = n_1 - j\kappa_1$ is the complex refractive index of the metal; ε_2 is the angle of refraction (viewing). The resulting radiation coefficient ε is the average value of the parallel and perpendicular components:

$$\varepsilon = \frac{1}{2}(\varepsilon_\parallel + \varepsilon_\perp). \qquad (16)$$

The degree of radiation polarization is defined as

$$P_E(\varepsilon_v) = \frac{\varepsilon_\perp(\varepsilon_v) - \varepsilon_\parallel(\varepsilon_v)}{\varepsilon_\perp(\varepsilon_v) + \varepsilon_\parallel(\varepsilon_v)}, \qquad (17)$$

where $\varepsilon_v = \varepsilon_2$ is the viewing angle.

Most drone bodies are made of foam plastic, which is an opaque dielectric and has a reflection coefficient R_1=0.8, or aluminum, which has a complex refractive index n_c=4,45-j3,3 [7, 11].

The dependence of the partial radiation coefficients $\varepsilon_\parallel(\varepsilon_v)$ and $\varepsilon_\perp(\varepsilon_v)$ and the degree of polarization $DOP(\varepsilon_v)$ at the aluminum-air interface on the viewing angle ε_v is shown in Fig. 7. For aluminum surface radiation, the parallel component is greater than the perpendicular component. The parallel component increases with increasing viewing angle to a maximum value of about 0.9, and then decreases at large angles. The perpendicular component decreases monotonically with increasing angle ε_v. The total radiation coefficient ε increases slightly with increasing angle ε_v. The degree of polarization increases with increasing viewing angle to a maximum value of 92% at $\varepsilon_v \approx 90$. When constructing graphs to take into account the roughness and oxidation of the aluminum plate surface, the complex refractive index $n_c = 4,45 - j3,3$.

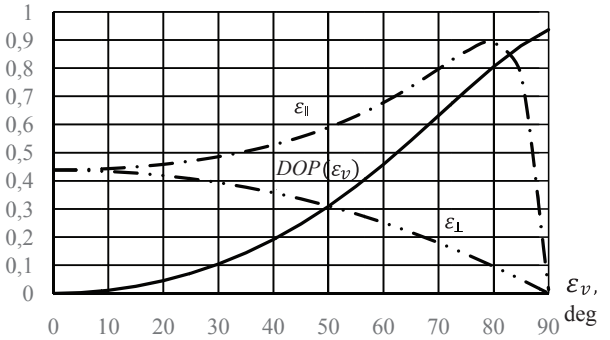

Fig. 7. Dependence of partial radiation coefficients and degree of polarization of aluminum surface radiation on the viewing angle ε_v at $n_c = 4,45 - j3,3$

Analysis of the laws of thermal radiation of the aluminum surface shows:

1. The radiation is partially polarized, which is due to the difference in the radiation coefficients for linearly polarized light in the plane of observation $\varepsilon_{\parallel}$ and the plane perpendicular to it $\varepsilon_{\perp}$.

2. The perpendicular component of linearly polarized radiation $E_{\perp}(\varepsilon_v)$ in the plane of observation with an increase in the angle of observation monotonically decreases from 0.44 at $\varepsilon_v = 0°$ to zero at $\varepsilon_v = 90°$.

3. The parallel component of linearly polarized radiation $E_{\parallel}(\varepsilon_v)$ in the plane of observation with an increase in the viewing angle ε_v increases from 0.44 to a maximum value of 0.9 at $\varepsilon_v \approx 80$, and then decreases to zero at $\varepsilon_v = 90°$.

4. The degree of polarization $DOP(\varepsilon_v)$ of the radiation of the aluminum surface with an increase in the viewing angle ε_v increases from zero to a maximum value of 0.93 at $\varepsilon_v \approx 90°$.

5. For small viewing angles $\varepsilon_v < 30$, which is typical for typical observation cases, the degree of polarization does not exceed 10%, and the resulting radiation coefficient $\varepsilon \approx \varepsilon_{\parallel} \approx \varepsilon_{\perp} = 0,438$.

4 Polarization of reflected thermal radiation

The theory of polarization of reflected external IR radiation is based on Fresnel's formulas, which allow calculating the energy coefficients of reflection of natural and linearly polarized light depending on the angle ε_1 of incidence of the beam on the reflecting surface [10, 11].

Electromagnetic radiation incident on the surface of an object is reflected and absorbed differently depending on the refractive index of the object. Will consider the electric field intensity vector of the incident radiation in the form of two plane-polarized components: the incident radiation can be considered to consist of a component $E_{\parallel}$, which is parallel to the plane of incidence, and a component $E_{\perp}$, which is perpendicular to the plane of incidence. These components interact differently with the surface, generating different reflection and absorption properties of the component $E_{\parallel}$ and the component $E_{\perp}$, respectively, which in turn generates the polarization state of the radiation emitted from the surface.

Fresnel reflection coefficients can be calculated the theory of Born and Wolf [10] using the complex refractive index of the medium $n_c(\lambda) = n(\lambda) + j\kappa(\lambda)$. These coefficients were obtained under the assumptions:

1. Objects can be considered as flat surfaces with uniform refractive indices.

2. The radiation environment in which the object is located can be considered as a homogeneous hemispherical black body with an unknown temperature.

3. The refractive index of air is equal to one.

For practical application of the formulas given in monograph [11], their approximate form is used [12]

$$R_{\perp} = R_s = \left(\frac{E_{sr}}{E_{si}}\right)^2 = \left[\frac{(n_2 - \cos\varepsilon_1)^2 + (\kappa n_2)^2}{(n_2 + \cos\varepsilon_1)^2 + (\kappa n_2)^2}\right]; \quad (18)$$

$$R_{\parallel} = R_p = \left(\frac{E_{pr}}{E_{pi}}\right)^2 = \frac{\left(n_2 - \frac{1}{\cos\varepsilon_1}\right) + (\kappa n_2)^2}{\left(n_2 + \frac{1}{\cos\varepsilon_1}\right) + (\kappa n_2)^2}. \quad (19)$$

In practice, simpler Fresnel formulas are used [12]

$$R_{\parallel} = \left|\frac{n_2\cos\varepsilon_1 - n_2\cos\varepsilon_2}{n_2\cos\varepsilon_1 + n_1\cos\varepsilon_2}\right|^2; \quad (20)$$

$$R_{\perp} = \left|\frac{n_1\cos\varepsilon_1 - n_1\cos\varepsilon_2}{n_1\cos\varepsilon_1 + n_2\cos\varepsilon_2}\right|^2, \quad (21)$$

where $R_{\parallel}$ and $R_{\perp}$ represent the energy reflection coefficients of the parallel and perpendicular components; E_{pi} and E_{si} are the electric field intensities of the incident light in the parallel and perpendicular directions; E_{pr} and E_{sr} are the electric field intensities of the reflected light in the parallel and perpendicular directions; n_1 is the refractive index of the medium for the incident ray; n_2 is the refractive index of the medium for the refracted ray; ε_1 is the angle of incidence, and ε_2 is the angle of refraction. The resulting reflection coefficient R is the average value of the parallel and perpendicular components

$$R = \frac{1}{2}(R_{\parallel} + R_{\perp}). \quad (22)$$

The degree of polarization of radiation is defined as

$$P_R(\varepsilon_v) = \frac{R_{\perp}(\varepsilon_v) - R_{\parallel}(\varepsilon_v)}{R_{\perp}(\varepsilon_v) + R_{\parallel}(\varepsilon_v)}, \quad (23)$$

where $\varepsilon_v = \varepsilon_1$ is the viewing angle.

Most drone bodies are made of foam plastic, which is an opaque dielectric with a reflection coefficient of R_1=0.8, or aluminum, which has a complex refractive index of $n_c = 4,45 - j3,3$ [16].

The dependence of the partial reflection coefficients $R_{\parallel}(\varepsilon_v)$ and $R_{\perp}(\varepsilon_v)$ and the degree of polarization $DOP(\varepsilon_v)$ at the air-aluminum interface on the viewing angle ε_v is shown in Fig. 8.

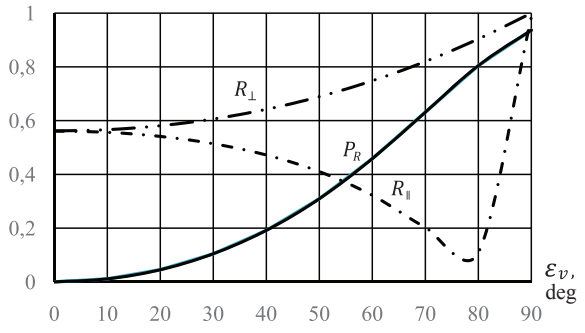

Fig. 8. Dependence of the partial reflection coefficients of the aluminum surface and the degree of radiation polarization on the angle ε_v at $n_c = 4,45 - j3,3$

For aluminum surface radiation, the perpendicular component is greater than the parallel component. The parallel component decreases with increasing viewing angle to a minimum value of about 0.09, and then increases at large angles. The perpendicular component increases monotonically with increasing angle ε_v. The degree of polarization increases with increasing viewing angle to a maximum value of 92% at $\varepsilon_v \approx 90°$. When constructing graphs the roughness and oxidation of the aluminum plate surface, a complex refractive index $n_c = 4,45 - j3,3$.

5 Physical and mathematical model of drone radiation polarization

The same test objects are used to research different types of TIMS, which allows comparing the characteristics of different thermal imagers. The main requirements for test objects are adequacy to real observation objects (targets), simplicity of the model and its implementation, and the ability to change the initial spatial and energy parameters.

The most common model is the BTS model for testing thermal imagers of armored vehicles [17,18]. In 1995, the North Atlantic Treaty Organization (NATO) adopted Agreement 4347 on standardization for land forces, "Determination of nominal characteristics of static range for infrared observation systems".

NATO Standard 4347 defines the static range characteristics of an TIMS when there is no search, the target is in the system's field of view, and the operator has unlimited time to detect the target. The standard applies only to IR surveillance systems that meet the minimum resolution temperature difference (MRTD) characteristics and is used for ground applications. The spectral ranges 3...5, 8...14 μm or part of these ranges.

The test object is a metal plate with a size of $V_t \times W_t = 2,3 \times 2,3$ m^2, the surface of which radiates as a black body (BB) and has a temperature contrast between the object and the background (relative to the CBB temperature of 288 K) $\Delta T_o = 2$ K.

5.1 Drone surface model

Similar to NATO standard 4347, offer a drone model in the form of a rectangular aluminum plate with dimensions corresponding to the effective dimensions of the drone. The surface of the plate has an average reflectance coefficient of $R = 0,92$ and a complex refractive index of $n_c = 4,45 - j3,3$. The plate is installed in front of a background emitter in the form of an aluminum plate that emits as black body and has a temperature of 288 K.

5.2 Polarization model combining reflection and emission effects

The surface of the plate simultaneously reflects and emits light energy, but these two radiation effects have opposite properties with respect to polarization. Therefore, it is these effects that determine the resulting polarization of IR radiation. The degree of polarization of such radiation can be determined using the equation:

$$P_{RS} = \left| \frac{L_{RS\parallel} - L_{RS\perp}}{L_{RS\parallel} + L_{RS\perp}} \right|, \tag{24}$$

where $L_{RS\parallel}$ is the resulting brightness of reflected and emitted radiation in a parallel plane; $L_{RS\perp}$ is the resulting brightness of reflected and emitted radiation in a perpendicular plane. If the surface of the plate emits radiation according to the Buge-Lambert law, they can be calculated using the formulas:

$$\begin{aligned} L_{RS\parallel} &= \frac{1}{\pi}\left(R_\parallel E_e + \varepsilon_\parallel M_{BB}\right); \\ L_{RS\perp} &= \frac{1}{\pi}\left(R_\perp E_e + \varepsilon_\perp M_{BB}\right), \end{aligned} \tag{25}$$

where E_e is the illuminance of the plate surface formed by external radiation (e.g., the Sun E_{Su}) and the atmosphere E_a: $E_e = E_{Su} + E_a$; M_{BB} is the integral luminance of the black body with a temperature equal to the temperature T of the drone model [12]:

$$M_{BB}(T) = \int_{\lambda_1}^{\lambda_2} \frac{c_1}{\lambda^5 \left[exp\left(\frac{c_2}{\lambda T}\right) - 1\right]} d\lambda, \ \frac{\text{W}}{\text{cm}^2}, \tag{26}$$

where $c_1 = 37415$ W $\cdot$ cm$^{-2}\cdot$ μm^4, c_2=14388 μm $\cdot$ K – constant coefficients; λ – wavelength, μm; $\lambda_1 \ldots \lambda_2$ – working spectral range of the thermal imager, μm.

Consider the brightness ratio of a plate formed by emission radiation L_E to the brightness of reflected radiation L_R

$$\begin{aligned} K_L = \frac{L_E}{L_R} &= \frac{M_{BB}(\varepsilon_\parallel + \varepsilon_\perp)}{E_e(R_\parallel + R_\perp)} = \\ &= \frac{(\varepsilon_\parallel + \varepsilon_\perp)}{(E_{Su} + E_a)(R_\parallel + R_\perp)} \int_{\lambda_1}^{\lambda_2} \frac{c_1}{\lambda^5 \left[exp\left(\frac{c_2}{\lambda T}\right) - 1\right]} d\lambda. \end{aligned} \tag{27}$$

The degree of polarization of the resulting radiation (24), taking into account (25), is defined as

$$
\begin{aligned}
P_{RS} &= \left|\frac{L_{RS\parallel} - L_{RS\perp}}{L_{RS\parallel} + L_{RS\perp}}\right| = \\
&= \left|\frac{\frac{1}{\pi}(R_\parallel E_e + \varepsilon_\parallel M_{BB}) - \frac{1}{\pi}(R_\perp E_e + \varepsilon_\perp M_{BB})}{\frac{1}{\pi}(R_\parallel E_e + \varepsilon_\parallel M_{BB}) + \frac{1}{\pi}(R_\perp E_e + \varepsilon_\perp M_{BB}}\right| = \\
&= \left|\frac{E_e(R_\parallel - R_\perp) + M_{BB}(\varepsilon_\parallel - \varepsilon_\perp)}{E_e(R_\parallel + R_\perp) + M_{BB}(\varepsilon_\parallel + \varepsilon_\perp)}\right| = \\
&= \left|\frac{(\varepsilon_\perp - \varepsilon_\parallel) + K_L(\varepsilon_\parallel - \varepsilon_\perp)}{(R_\parallel + R_\perp) + K_L(\varepsilon_\parallel + \varepsilon_\perp)}\right| = \\
&= \left|\frac{(\varepsilon_\perp - \varepsilon_\parallel)(1 - K_L)}{2 - (\varepsilon_\parallel + \varepsilon_\perp) + K_L(\varepsilon_\parallel + \varepsilon_\perp)}\right| = \\
&= \left|\frac{(\varepsilon_\perp - \varepsilon_\parallel)(1 - K_L)}{2 - (\varepsilon_\parallel + \varepsilon_\perp)(-1 + K_L))}\right| = \\
&= \left|\frac{(\varepsilon_\perp - \varepsilon_\parallel)(1 - K_L)}{2 + (\varepsilon_\parallel + \varepsilon_\perp)(1 - K_L)}\right|.
\end{aligned}
\tag{28}
$$

Simulation of the polarization degree curves of the radiation from the surface of an aluminum plate, taking into account formulas (25) and (26) at different values of K_L, is shown in Fig. 9. If the polarization degree is $P_{RS} > 0$, then such radiation has parallel polarization, and if $P_{RS} < 0$, then such radiation has perpendicular polarization.

The resulting formula (28) shows that the degree of polarization is determined by the value of the coefficient K_L. When K_L is less than one, the reflected radiation is greater than the emitted radiation. If K_L is greater than one, this means that the emitted radiation is greater than the reflected radiation. When the value of K_L is greater than one, the polarization degree modulus increases with an increase in K_L.

5.3 Analysis of the results

To research polarimetric thermal imagers, it was proposed to use a test object in the form of a flat aluminum plate with a complex refractive index of $n_c = 4,45 - j3,3$.

Methods for calculating the polarization characteristics of radiation from thermal objects were considered, and the research showed that:

- The radiation itself is partially polarized due to differences in the radiation coefficients of the object's surface for two linearly polarized waves in mutually perpendicular planes.
- Reflected external radiation is also partially polarized due to differences in the reflection coefficients of the object surface for two linearly polarized waves in mutually perpendicular planes.
- To model the polarization state of the radiation of the observed object, it is advisable to select the image intensity, degree of polarization, and polarization angle, which are determined by the Stokes parameters.

Analysis of the results obtained shows that:

1. For thermal radiation at observation angles $\varepsilon_v < 30°$, the components of the radiation coefficient are almost equal $\varepsilon_\parallel \approx \varepsilon_\perp \approx 0,45$, but $\varepsilon_\parallel > \varepsilon_\perp$. With an increase in the observation angle $\varepsilon_v > 30$, the perpendicular polarization component $\varepsilon_\perp$ monotonically decreases to zero, and the parallel component $\varepsilon_\parallel$ increases and reaches a maximum value of 0.92 at an angle $\varepsilon_v > 78°$, and then decreases to zero. The degree of polarization of radiation increases with increasing angle ε_v and at an angle 78° is equal to 0.79.

2. The reflection coefficient at normal incidence is 0.92. For any angle, the perpendicularly polarized component is greater than the parallel component. The parallel component has a minimum equal to 0.08 at an angle of incidence of 78°. For this angle, the degree of polarization of the reflected radiation is equal to 0.49.

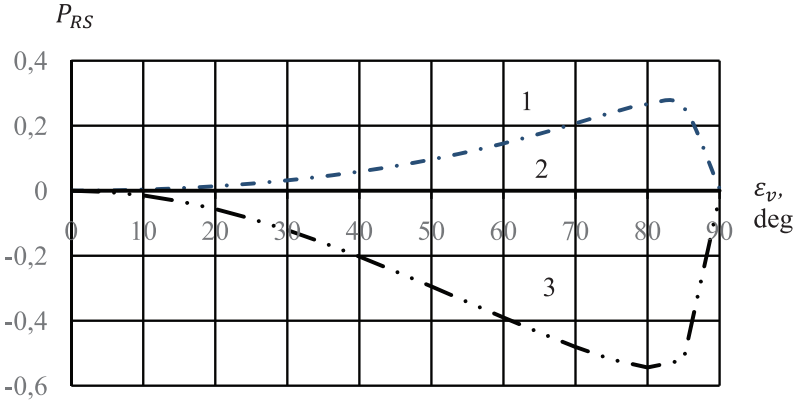

Fig. 9. Dependence of the degree of polarization of the test object's radiation on the viewing angle ε_v, when the ratio K_L of the brightness of the plate formed by emission radiation L_E, to the brightness of the reflected radiation L_R is equal to: 1 – 0.8; 2 – 1.0; 3 – 1.3

Conclusions

A physical and mathematical model of polarized infrared radiation of a drone test object has been developed and investigated, which can be used in the creation of polarimetric thermal imagers designed to detect and recognize drones. The polarization of radiation is based on two main theories: Fresnel's theory and Kirchhoff's law, which are determined only by the refractive indices of the media. In most cases, the infrared radiation of objects (targets) and backgrounds can be partially polarized and natural.

To research such radiation according to the Stokes method, an optical system was selected that converts this radiation into elliptically polarized radiation. The intensity parameters of this radiation allowed the development of a method for calculating the intensity, degree of polarization, azimuth, and ellipticity of polarization using the Stokes vector.

The use of the polarization properties of IR radiation for the visualization of thermal objects allows the creation of a new class of high-precision optoelectronic devices — polarimetric thermal imagers. An analysis of scientific and technical literature has shown that significant research on the creation of polarimetric thermal imagers (PTI) is being conducted in military laboratories in the United States and China. The fundamental difference between classic thermal imagers, which convert the distribution of infrared brightness of the target and background into a visible analogue of this distribution (image) on the display screen, is that PTI use differences in the polarization characteristics of the target and background radiation, such as intensity, degree of polarization, azimuth, and polarization ellipticity. This makes it possible to significantly increase the range of target detection and recognition, as well as to observe targets in the absence of radiation (temperature) contrast.

It is proposed to calculate the polarization state of reflected or emitted IR light (energy brightness, luminosity, illuminance), which determines the background-target environment (BTS), using Stokes parameters. The Stokes parameters were determined through the components of the electric field E_{0x} and E_{0y} the phase difference between two orthogonal electric field intensities $\vec{E}_x \perp \vec{E}_y$, and the Stokes parameters themselves are calculated for each pixel of the matrix radiation detector (MRD).

To research and design such polarimetric thermal imagers, a physical and mathematical model of radiation polarization from observation objects is considered, which takes into account the polarization properties of intrinsic thermal radiation and reflected external radiation. As a result of researching this model, it was established that:

1. Intrinsic radiation is partially polarized due to differences in the radiation coefficients of the object surface for two linearly polarized waves in mutually perpendicular planes. The research of the components of the radiation coefficients showed that the component for a wave polarized in the plane of incidence is smaller than the component polarized in the perpendicular plane.

2. Reflected external radiation is also partially polarized due to differences in the reflection coefficients of the object surface for two linearly polarized waves in mutually perpendicular planes. Moreover, the component polarized in the plane of incidence is always smaller than the component polarized in the perpendicular plane.

3. A fundamental feature of the polarization properties of IR radiation from objects and backgrounds due to their own and reflected radiation is that they are opposite in nature, which significantly worsens the resulting degree of polarization.

4. The results of the research should be used in the development of a test object model, which is necessary for the design of a polarimetric thermal imager.

5. For further research, it is advisable to conduct experimental measurements of the polarization of infrared radiation from real drones and the atmosphere, which will allow refining the parameters of the test object.

References

[1] Schuster, N. & Kolobrodov V. G. (2004). *Infrarot thermographie*. Zweite, überarbeitete und erweiterte Ausgabe, WILEY-VCH, 356 p.

[2] Richard Johnson. (2025). *Drone Systems and Operations: Definitive Reference for Developers and Engineers*. HiTeX Press, 479 p.

[3] Vollmer M., Mollman K.-P. (2018). Infrared Thermal Imaging. Fundamentals, Research and Applications. Second Edition. *Wiley – VCH*, pp. 788. DOI: 10.1002/9783527693306.

[4] Li, X., Yan, L., Qi, P., Zhang, L., Goudail, F., Liu, T., et al. (2023). Polarimetric Imaging via Deep Learning: A Review. *Remote Sensing*, Vol. 15, Iss. 6, 1540. DOI: 10.3390/rs15061540.

[5] Zhang Y., Shi Z., Qiu T. (2017). Infrared small target detection method based on decomposition of polarization information. *Journal of Electronic Imaging*, Vol. 26, Iss. 3, 033004. DOI: 10.1117/1.JEI.26.3.033004.

[6] Goldstein D. H. (2011). Polarized Light. Third edition. *CRC Press, Taylor & Francis Group*, 786 p. DOI: 10.1201/b10436.

[7] Russell Chipman, Wai Sze Tiffany Lam, Garam Young (2019). Polarized Light and Optical Systems. *Taylor & Francis, CRC Press*, 982 p. DOI: 10.1201/9781351129121.

[8] Kolobrodov V. G., Mykytenko V. I., Pinchuk B. Yu., Sokol B. V., Tiagur V. M. (2021). Computer-Integrated Method of Object Detection by Thermal Polarimetric Imager. *Visnyk NTUU KPI Seriia - Radiotekhnika Radioaparatobuduvannia*, Vol. 85, pp. 21-25. DOI: 10.20535/RADAP.2021.85.21-26.

[9] Zhang, Y., Fu, Q., Luo, K., Yang, W., Zhan, J., et al. (2023). Analysis of Two-Color Infrared Polarization Imaging Characteristics for Target Detection and Recognition. *Photonics*, Vol. 10, No. 11, 1181. DOI: 10.3390/photonics10111181.

[10] Kolobrodov V. G. (2020). *Fundamentals of Wave Optics*. Kyiv: Igor Sikorsky Kyiv Polytechnic Institute, Polytechnika Publishing House, 404 p. ISBN 978-966-990-017-3.

[11] Born M., Wolf E. (2020). *Principles of Optics*, 7th edn. Cambridge University Press, 7th edition, 952 p.

[12] Zhang J.-H., Zhang Y., Shi Z.-G. (2018). Enhancement of dim targets in a seabackground based on long-wave infrared polarisation features. *IET Image Process.*, Vol. 12, Iss. 11, pp. 2042-2050. DOI: 10.1049/iet-ipr.2018.5607.

[13] Herbert Kaplan. (2007). Practical Applications of Infrared Thermal Sensing and Imaging Equipment. 3rd ed. *SPIE Press*, 236 p., DOI: 10.1117/3.725072.

[14] Liu H., Li X., Wang Z., et al. (2024). Review of polarimetric image denoising. *Advanced Imaging*, Vol. 1, Iss. 2, 022001-20. DOI: 10.3788/AI.2024.20001.

[15] Aron, Y., Gronau, Y. (2005). Polarization in the LWIR: a method to improve target aquisition. *Proc. SPIE*, Vol. 5783, pp. 653-661. DOI: 10.1117/12.605316.

[16] Introduction to Polarization. *Edmund Optics*, access data: September, 2025.

[17] STANAG No. 4348, Definition of nominal static range performance for image intensifier systems, 1988.

[18] Chrzanowski K. (2010). *Testing thermal imagers. Practical guidebook*. Military University of Technology, 00-908 Warsaw, Poland, 164 p.

[19] McVay, J. A., Mclemore, D. P., Stubbs, J. J. (2019). Polarized Radar for Detection and Automatic Non-Visual Assessment of Unmanned Aerial Systems. *OSTI.GOV*, Report of Sandia National Laboratories Albuquerque, New Mexico (USA), 55 p.

Модель поляризації інфрачервоного випромінювання дрона

Колобродов В. Г.

Розроблено фізико-математичну модель поляризації інфрачервоного (ІЧ) випромінювання дрона, яку можна використовувати при створенні поляриметричних тепловізорів (ПТ), призначених для виявлення і розпізнавання об'єктів спостереження.

Аналіз і постановка задачі досліджень. Тепловізійні системи спостереження знаходять широке застосування, насамперед, у військовій справі, наприклад, як тепловізійні камери дронів. Принцип роботи класичних тепловізорів ґрунтується на перетворенні яскравості ІЧ випромінювання об'єкта спостереження і фону із площини предметів в адекватний розподіл яскравості зображення фоново-цільової обстановки на екрані дисплея у видимій області спектра. За незначного контрасту, або його відсутності, виявити такий об'єкт неможливо. Сучасні моделі не враховують одночасно власне і відбите випромінювання дрона, що призводить до помилкового визначення дальності виявлення. Використання поляризаційних властивостей випромінювання дозволяє вирішити цю проблему. Тому розробка і дослідження моделі поляризації ІЧ випромінювання дрона є дуже важливою задачею для створення перспективних поляриметричних тепловізорів.

Виділення невирішених частин загальної проблеми – відсутність моделі, яка одночасно враховує поляризації емісійного і відбитого випромінювання. *Ціль статті* полягає в розробці фізико-математичної моделі поляризації ІЧ випромінювання дрона, яку можна використовувати при створенні ПТ, призначених для виявлення і розпізнавання об'єктів.

Матеріал дослідження – модель дрона розглядалася як плоска пластина, яка характеризується коефіцієнтом відбивання і комплексним показником заломлення, що дозволило розробити методи розрахунку параметрів еліптично поляризованого випромінювання. Аналіз розроблених методів показав, що для моделювання поляризаційного стану випромінювання об'єкта спостереження доцільно обирати інтенсивність зображення, ступінь поляризації і поляризаційний кут, які визначаються параметрами Стокса. Відмінність отриманих результатів полягає в науковому обґрунтуванні явища, що поляризація ІЧ випромінювання об'єктів і фонів за рахунок власного і відбитого випромінювання мають протилежний характер, що значно погіршує результуючу ступінь поляризації.

Висновки. Отримані результати досліджень доцільно використовувати при розробці моделі тест-об'єкта, яка необхідна при проєктуванні ПТ. Для подальших досліджень доцільно провести експериментальні вимірювання поляризації ІЧ випромінювання реальних дронів і атмосфери, які дозволять уточнити параметри тест-об'єкта.

Ключові слова: тепловізор; поляризація; ступінь поляризації; емісійне теплове випромінювання; відбите теплове випромінювання